A Microscopic Interpretation of the RF Noise Performance of Fabricated FDSOI MOSFETs

Raúl Rengel, María Jesús Martín, Tomás González, *Member, IEEE*, Javier Mateos, Daniel Pardo, Gilles Dambrine, *Member, IEEE*, Jean-Pierre Raskin, *Member, IEEE*, and François Danneville, *Member, IEEE*

***Abstract*—In this paper, a detailed research of the high-frequency noise sources and figures of merit (FOMs) of fabricated deep-submicrometer n-channel fully depleted silicon-on-insulator MOSFETs is carried out. Special care is given to reproduce the main topology parameters, together with the most relevant parasitic elements of real devices in order to accomplish an accurate and reliable simulation. The information provided by the Monte Carlo (MC) tool allows getting a physical insight of the relationship between internal quantities and the main noise sources inside the device; moreover, the spectral density of velocity fluctuations has been analyzed spatially in order to determine the local current noise source in the gradual channel and velocity overshoot sections of the effective channel. Together with the calculation of intrinsic noise sources, the MC simulator is able to reproduce the measurements for the main noise FOMs in the RF and microwave frequency ranges. Moreover, the whole simulation framework allows addressing the importance of parasitic elements in the final value of these FOMs.**

***Index Terms*—Fully depleted silicon-on-insulator (FD-SOI), high-frequency noise, minimum noise figure, Monte Carlo (MC) simulation, MOSFET, parasitic resistances, velocity fluctuations.**

I. Introduction

In TODAY'S wireless world, silicon CMOS devices for analog RF applications may play a crucial role for a feasible development of low-cost high-frequency designs [1], [2]. Silicon-on-insulator (SOI) technology [3] has recently emerged as the most reasonable solution to the problems of traditional bulk devices when the size of the transistors reaches very small dimensions [4], [5]. In order to fully profit and extend the advantages provided by SOI transistors, it is necessary to develop models and design tools specifically adapted for these devices. In particular, an accurate modeling of high-frequency noise is essential. In the last years, many efforts have been devoted to the modeling of high frequency noise in deep-submicrometer MOSFET devices see, i.e., [6]–[11]. Specifically, models incorporating so-called physical noise sources are of significant importance when dealing with short-channel devices. Due to its stochastic nature, the ensemble Monte Carlo (MC) method [12] is a highly interesting alternative for the study of noise phenomena. This modeling methodology intrinsically incorporates all the transport processes of importance in small devices (including far-from-equilibrium phenomena, such as nonstationary effects or the appearance of hot carriers) and makes no assumption about the physical origin of noise sources. These are provided in a natural way by means of the fluctuations of carrier velocity generated by scattering mechanisms in the simulation. In this way, an MC device simulator can be considered as a global noise modeling tool, providing from local noise velocity fluctuations to noise spectra of current fluctuations at terminals and the main noise circuital parameters such as the minimum noise figure. This modeling approach has been widespread used for the study of noise in semiconductor materials, III-V FET devices, n^+-n-n^+ structures, diodes, BJTs, etc. However, to the authors' knowledge, it has been barely considered in the literature for an overall investigation (from microscopic noise sources to circuital noise parameters) of high-frequency noise in MOSFETs.

In the present work, we analyze the information provided by our in-house MC simulator in order to investigate the high-frequency noise behavior of fabricated fully depleted (FD) SOI MOSFETs. The paper is organized as follows: in Section II details are given about the devices under test and the MC procedure for the study of high-frequency noise. In Section III the main noise results are presented. First, the spectral density of drain current fluctuations in the microwave range is analyzed for various bias conditions. The noise spectra of velocity fluctuations of carriers in different regions of the channel (dividing the channel in two different areas by considering the location were the saturation velocity corresponding to bulk material is surpassed) are also investigated. Afterwards, we shall focus on the study of the noise through the normalized intrinsic parameters α, β and C. Finally, the most important parameters from the experimental and circuital point of view, such as the minimum noise figure ($\mathrm{NF}_{\min}$), associated gain (G_{ass}), noise resistance (R_n) and optimum reflection coefficient (Γ_{opt}) are studied taking into account the effects associated to parasitic elements. Experimental values and numerical calculations will be compared. In Section IV the main conclusions of our work will be presented.

II. Fabricated Devices and MC Procedure

The FD SOI n-MOSFET devices under test were fabricated on 200-mm diameter UNIBOND wafers by means of a CMOS-compatible process. The effective gate length is 160 nm, and the thickness of the active layer is 30 nm, which ensures the full depletion condition in the channel. The buried oxide thickness is

Manuscript received September 13, 2005; revised November 21, 2005. This work was supported in part by the "Consejería de Educación de la Junta de Castilla y León" under Research Project SA008B05. The review of this paper was arranged by Editor M. J. Deen.

R. Rengel, M. J. Martín, T. González, J. Mateos, and D. Pardo are with the Departamento de Física Aplicada, Universidad de Salamanca, Salamanca 37008, Spain (e-mail: raulr@usal.es).

G. Dambrine and F. Danneville are with the Département Hyperfréquences et Semiconducteurs, IEMN, Villeneuve d'Ascq, Cedex F-59655, France.

J.-P. Raskin is with the Microwave Laboratory, Université catholique de Louvain, Louvain-la-Neuve B-1348, Belgium.

Digital Object Identifier 10.1109/TED.2005.863541

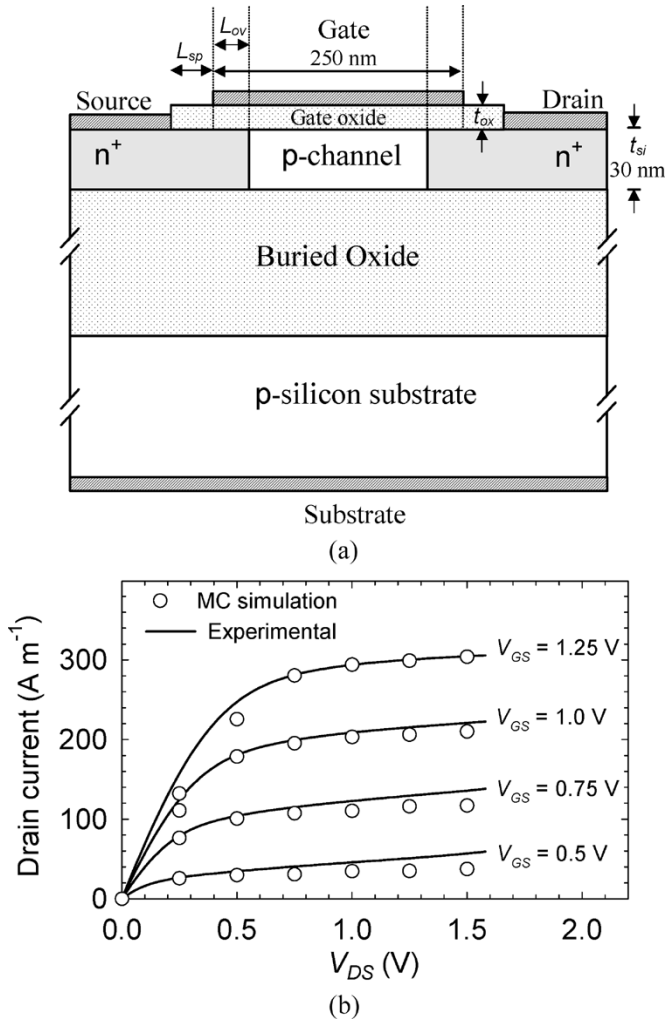

Fig. 1. (a) Scheme of the simulated devices and (b) output characteristics for various gate voltages.

400 nm and the total device width (W) is 100 μm. More details about the fabrication and parameters of the devices can be found in [13], [14].

The simulated structure [Fig. 1(a)] reproduces most of the topology parameters in their actual values. The gate oxide thickness is 5.5 nm, the overlap length has been estimated to be 45 nm and the spacer length is 80 nm. The doping concentration of the p substrate in the active layer is $8 \cdot 10^{17}$ cm^{-3} and the doping of the n$^+$ regions at the drain and source spacer and overlap areas is $2 \cdot 10^{18}$ cm^{-3}. Numerical calculations have been performed by using a two-dimensional ensemble MC simulator. The main features of the simulator and the parameters considered for the physical model can be found in [14]–[17]. The dynamic behavior of the devices under study was presented in detail in a previous work [14]; a good agreement was found between experimental data and simulation results for the main dynamic figures of merit (FOMs) thanks to the careful consideration of the topology of the devices and the extrinsic parasitics as well as the access feed lines, which confirmed in a first step the validity of the modeling approach. Fig. 1(b) shows the output characteristics (experimental measurements together with MC simulations) for different gate voltages ranging from 0.5 to 1.25 V.

Regarding noise calculations, several considerations must be pointed out. As the purpose of our work is the characterization of the noise performance of the devices at high frequency, we chose a typical noisy two-port device representation: the noiseless device is represented by a "black box" (described by admittance parameters), and two current noise generators are considered, one at the input (gate) and the other at the output (drain), both correlated [18]. These noise sources can be determined by the EMC procedure without making any assumption about their physical origin, by means of the analysis of instantaneous current at terminals. Since the method provides the current fluctuations for each timestep, the correlation functions for gate and drain terminals (and the cross-correlation) can be calculated. Fourier transformation of these quantities allows the direct determination of the spectral densities of current fluctuations $S_{\rm IG}(f)$, $S_{\rm ID}(f)$ and $S_{\rm IGID}(f)$ (corresponding to the gate and drain and the cross-correlation between both) required for the two-port noise analysis previously mentioned. The combination of these quantities with the complex four admittance parameters gives the main circuital FOMs (minimum noise figure, associated gain, etc.).

Moreover, from the information provided by the simulator it is also possible to analyze the so-called velocity-fluctuation noise [18] by determining the spectral intensity of velocity fluctuations S_v (see Appendix I). In this way, the local noise source $S_{\rm in}$ can be investigated in different sections of the channel: in our case, we considered two subsections of the channel, the diffusive or gradual channel section, to which we will refer as Section I (where the average velocity is below $v_{\rm SAT}$, the saturation velocity in bulk material) and the overshoot section or Section II (where $v > v_{\rm SAT}$). Therefore, valuable information is obtained about the noisy nature of carriers in the overshoot section, a subject of controversy in the literature.

To ensure the validity of the calculations, an accurate evaluation of the instantaneous current fluctuations at source, drain and gate terminals is necessary: we used an adaptation of the Ramo–Shockley theorem for the calculation of these currents [19], [20]. When dealing with the comparison with experimental results, the effect of parasitics (that are provided by the experimental measurements in a procedure completely separated from numerical simulations) will be incorporated into the intrinsic MC results. In this way, the influence of parasitic elements on the final determination of the main noise FOMs can be readily evaluated. Moreover, the simulation results and the microscopic nature of the simulation approach allow bringing some understanding about the noise phenomena at high frequencies, as we shall see in the next section.

III. Noise Results

A. Intrinsic Current Noise Sources

Fig. 2 shows the values of $S_{\rm ID}$ as a function of frequency for $V_{\rm GS}$ ranging from 0.5 to 1.25 V and $V_{\rm DS} = 1.5$ V. As it can be observed, for frequencies up to 50 GHz, a white noise behavior is obtained. To achieve a correct determination of $S_{\rm ID}$ in this frequency range, it is necessary to solve the electric field in the simulation at each time step; in this way, the contribution of field fluctuations is properly taken into account. For higher values of

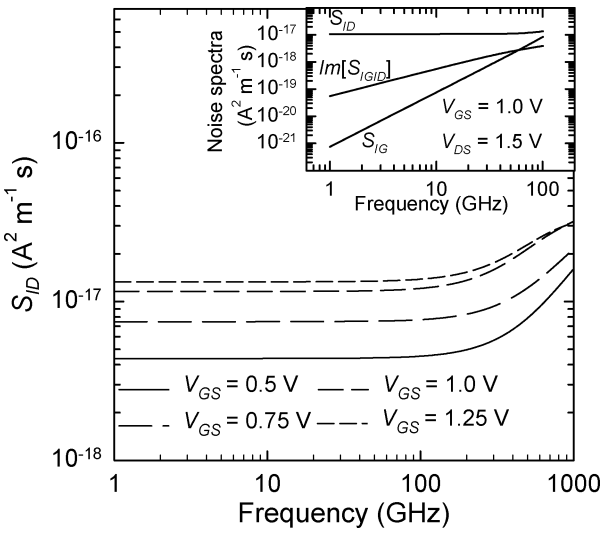

Fig. 2. Values of $S_{\rm ID}$ as a function of frequency for various gate bias in saturation ($V_{\rm DS} = 1.5$ V). The inset shows the frequency dependence of $S_{\rm ID}$, $S_{\rm IG}$ and $\rm Im[S_{IGID}]$ up to 50 GHz for $V_{\rm GS} = 1.0$ V and $V_{\rm DS} = 1.5$ V.

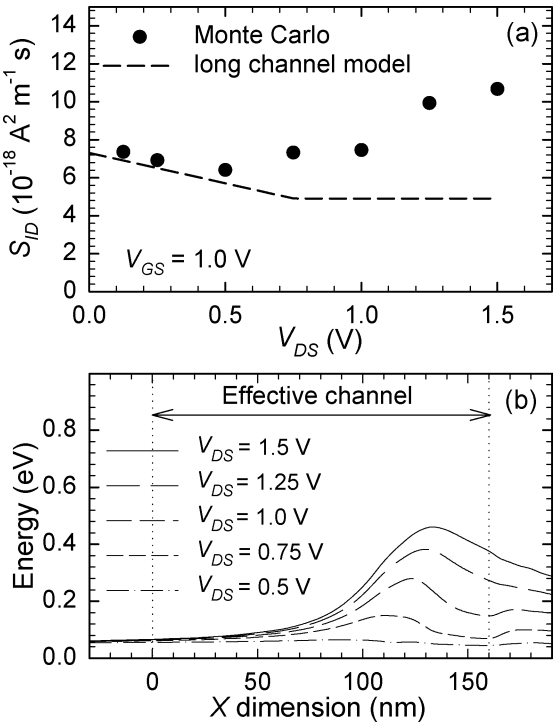

Fig. 3. (a) Values of $S_{\rm ID}$ as a function of $V_{\rm DS}$ for $V_{\rm GS} = 1.0$ V and (b) average values of electron energy along the channel for the same bias conditions.

frequency, $S_{\rm ID}$ tends to increase with f due to plasma oscillation phenomena, a fact that has been also observed in III-V FET devices and in BJTs and HBTs [21], [22]. The white noise behavior of $S_{\rm ID}$ in the gigahertz range evidences the velocity fluctuations of carriers as the primary origin of drain noise (in the absence of other noise processes not included in the model); in the next subsection, velocity-fluctuation noise will be the subject of analysis. From now on, we will focus on this "white noise" range; this is, up to 50 GHz (that includes the RF and microwave frequency ranges).

With regard to $S_{\rm IG}$, it exhibits f^2 dependence for these frequencies (see inset of Fig. 2). Its origin has been associated to the capacitive coupling to the gate of charge fluctuations within the channel; therefore, the primary origin of $S_{\rm IG}$ is the same, other than in the case of $S_{\rm ID}$. For the imaginary part of $S_{\rm IGID}$ a linear dependence with frequency is observed. The real part of $S_{\rm IGID}$ has been found to be much smaller than the imaginary part and it can be neglected in this frequency range. This behavior is in good agreement with the results predicted by the general theory for FETs [18] and in particular with the results previously observed in bulk MOSFETs [15].

We shall now focus on $S_{\rm ID}$, which is frequently considered as the primary intrinsic noise source in a MOSFET device from a circuital point of view. In Fig. 3(a) we show the values obtained for $S_{\rm ID}$ as a function of $V_{\rm DS}$ for $V_{\rm GS} = 1.0$ V. We have also plotted the results predicted by the theoretical Klaassen/van der Ziel's model [18], [23] (this is $S_{\rm ID} = 4\gamma g_{d0} K_B T$, the value for g_{d0}, extracted from the I_D–$V_{\rm DS}$ curve, was 435 S/m $^{-1}$, and γ varies from 1 for $V_{\rm DS} = 0.0$ V to 2/3 in saturation). As it can be observed, for values of $V_{\rm DS}$ lower than 0.5 V (corresponding to the triode regime), the drain noise generated by the device slightly decreases when $V_{\rm DS}$ increases, and it is in good agreement with the theoretical prediction. However, when reaching the saturation region (high $V_{\rm DS}$) an increase of $S_{\rm ID}$ with the drain bias is observed (in contrast with the theoretical model, which remains constant). This behavior has been also described by other authors attributing this augmentation of $S_{\rm ID}$ to channel length modulation (CLM) effects [8]. The nonlinearity within the channel provoked by the appearance of the pinch off is translated into a progressive stronger transfer to the drain terminal of the noise generated in the diffusive section as $V_{\rm DS}$ is raised (for fixed $V_{\rm GS}$), what would explain the increase of $S_{\rm ID}$.

However, it must be also noticed that, at high $V_{\rm DS}$ in saturation conditions the above mentioned nonlinearity of the channel yields to the appearance of high longitudinal electric fields near the drain and, as a consequence, free carriers present an important increase of energy in that area [Fig. 3(b)]. As $V_{\rm DS}$ is raised in saturation for constant $V_{\rm GS}$, the length of the overshoot section is wider and the maximum value of energy is higher. As it will be discussed in the next subsection, the local noise source $S_{\rm in}$ in the overshoot section also increases with $V_{\rm DS}$ and their values are similar to those of the diffusive section. For the device under test, noise generated by hot carriers near the drain could be also an important contributor to drain current noise [24], [25].

Let us now analyze the dependence of $S_{\rm ID}$ on the gate bias at a fixed $V_{\rm DS}$ equal to 1.5 V, in saturation conditions [Fig. 4(a)]. Together with the MC data, the results predicted for $S_{\rm ID}$ by Klaassen/van der Ziel's model [18], [23] are also shown. As it can be observed, the values obtained in the simulation are significantly higher than the theoretical prediction. Fig. 4(b) and (c) shows the values of electron energy and concentration in the inversion layer for various $V_{\rm GS}$ at the drain bias condition considered in Fig. 4(a). As $V_{\rm GS}$ is raised, the peak value of energy near the drain is decreased; in contrast, an increase of the average energy of carriers is detected in the rest of the channel, where the concentration of carriers is significant. Simultaneously, the average electric field in the diffusive region is raised, and the number of particles in the whole channel is increased.

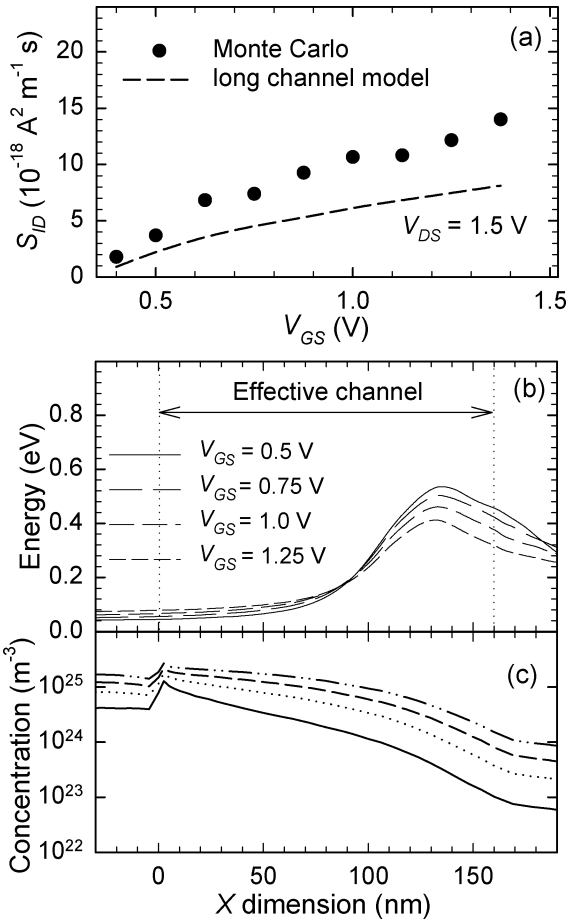

Fig. 4. (a) Values of $S_{\rm ID}$ as a function of $V_{\rm GS}$ for a fixed drain bias, (b) average values of energy, and (c) concentration of carriers along the channel for $V_{\rm DS} = 1.5$ V and various gate-to-source voltages.

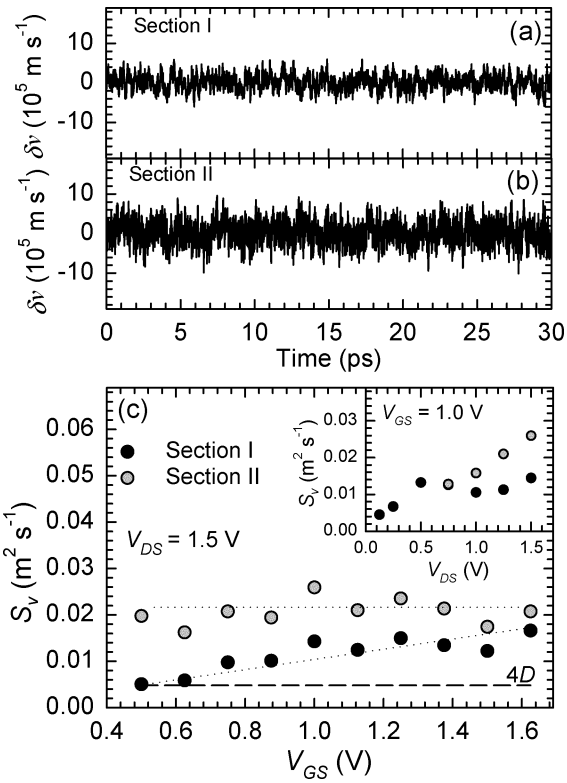

Fig. 5. Velocity fluctuations as a function of time in (a) Section I and (b) Section II for $V_{\rm GS} = 1.0$ V and $V_{\rm DS} = 1.5$ V. (c) S_v as a function of $V_{\rm GS}$ for fixed $V_{\rm DS} = 1.5$ V; tendency lines are included (dotted lines). Dashed line shows the value of S_v obtained from the bulk diffusion coefficient. Inset shows S_v as a function of $V_{\rm DS}$ for $V_{\rm GS} = 1.0$ V.

The combination of these facts produces an important augmentation of the local noise source within the channel, as it will be shown in the next subsection, thus producing the increase of $S_{\rm ID}$ with $V_{\rm GS}$.

B. Velocity Fluctuation Noise

According to the procedure indicated in Appendix I, we analyze the spectra of velocity fluctuations S_v in the diffusive and overshoot sections of the channel, what can provide useful information about the local current noise source. It is important to remark that we do no intend to "double calculate" $S_{\rm ID}$ by two separate methods: in fact, the determination of this quantity by means of the spectral density of velocity fluctuations would require in a second step to evaluate the transfer of the local noise source to the drain terminal through an impedance field [9]. The calculation of this impedance field by means of MC device simulation is neither affordable nor reliable from the practical point of view due to the stochastic nature of the simulation approach.

An example of velocity fluctuations (normalized to one particle) in the diffusive and overshoot sections can be observed in Fig. 5(a) and (b). As shown in the graph, the amplitude of fluctuations is much stronger in the overshoot section, what gives a higher zero-time value of the correlation function of the velocity fluctuations. Fig. 5(c) shows the results for S_v in Sections I and II as a function of $V_{\rm GS}$ for a fixed $V_{\rm DS} = 1.5$ V. In the graph, we have also plotted, as a reference, the low-field value of $4D$, D being the diffusion coefficient calculated in bulk material with analogous doping concentration as the substrate doping of the SOI structure. As it can be observed, the spectral intensity of velocity fluctuations, S_v, is much stronger in Section II (velocity overshoot) than in Section I (diffusive) especially for low $V_{\rm GS}$, this is, in deep saturation and near the weak inversion regime. As $V_{\rm GS}$ is increased, the difference between both sections is reduced: while S_v in Section II does not show a significant dependence on $V_{\rm GS}$, a progressive augmentation with the gate voltage is detected in Section I. This increase of S_v in Section I is mainly due to a larger zero-time value of the correlation function of velocity fluctuations (when $V_{\rm GS}$ is raised, the higher average longitudinal electric field in that area yields to a larger amplitude of velocity fluctuations), since the decay time of the correlation function does not vary significantly with $V_{\rm GS}$. In the case of Section II transport takes place under a quasi-ballistic regime, and once saturation conditions are reached for a given $V_{\rm DS}$ the values of S_v are not substantially modified when varying $V_{\rm GS}$.

It is noteworthy that, even in the case of Section I, in which the features of transport are closer to a diffusive regime, the values obtained for S_v are in general higher than the value predicted if considering the bulk diffusion coefficient through $S_v = 4D$. In this case, only for low $V_{\rm GS}$ (where the average energy of carriers is close to thermal equilibrium) a reasonable agreement is found between both calculations.

The inset of Fig. 5(c) shows S_v versus $V_{\rm DS}$ for the two sections of the channel considered. For low $V_{\rm DS}$, the device oper-

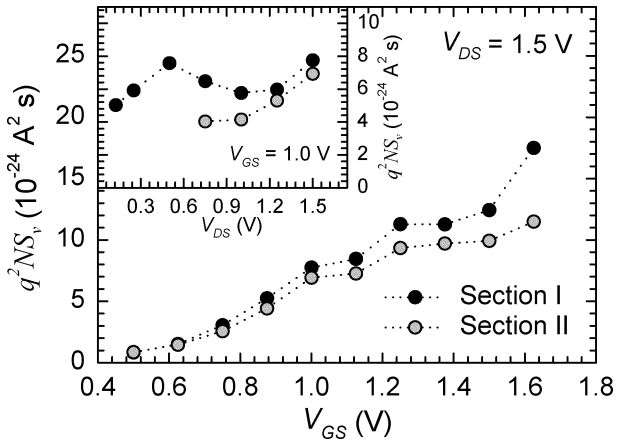

Fig. 6. $q^2\mathrm{NS}_v$ as a function of gate biasing for $V_{\mathrm{DS}} = 1.5\,\mathrm{V}$ in the two sections of the channel considered. Inset shows the results for $q^2\mathrm{NS}_v$ as a function of V_{DS} for $V_{\mathrm{GS}} = 1.0\,\mathrm{V}$.

ates in the triode regime, so the diffusive section in fact corresponds to the whole effective channel, where the device behaves practically like a linear resistor. At the beginning of saturation ($V_{\mathrm{DS}} = 0.75\,\mathrm{V}$), S_v is quite similar in both sections; nevertheless, when V_{DS} is increased S_v remains rather constant in Section I while it clearly augments in Section II. The increase of V_{DS} at fixed V_{GS} leads (once that saturation is reached) to the appearance of nonstationary phenomena and elevated longitudinal electric fields near the drain. As a consequence, carriers in Section II progressively reach elevated energies [Fig. 3(b)] and the ballistic character of transport intensifies in that area. From this result, the increase of S_{ID} versus V_{DS} in saturation [Fig. 3(a)] could be attributed to a stronger contribution of the noise generated in Section II. Nevertheless, it must be taken into account also that as V_{DS} is raised the length of Section I is decreased due to a stronger CLM effect: within the framework considered in this work a stronger impedance field in Section I provoked by CLM can not be discarded as the origin of current excess noise at the drain terminal.

To present a clearer idea of the local current noise source S_{in} in each subsection of the channel, in Fig. 6 we have represented the values of the $q^2\mathrm{NS}_v$ factor [see (A1) in the Appendix]. For both sections, an increase of $q^2\mathrm{NS}_v$ with V_{GS} is observed, what explains the augmentation of S_{ID} with the gate bias at fixed V_{DS} in saturation. In the case of Section II, the increase of $q^2\mathrm{NS}_v$ is due to the higher sheet carrier concentration N as V_{GS} is raised, while in Section I the increase of both N and S_v [Fig. 5(c)] combine to produce a finally slightly higher $q^2\mathrm{NS}_v$ factor than in the overshoot section. Checking the dependence on V_{DS}, shown in the inset, it can be observed how Section I presents a stronger value of $q^2\mathrm{NS}_v$, although at high V_{DS} (when carriers reach elevated energies) the results for the overshoot section are quite similar to those for the diffusive region.

C. α, β and C Parameters

Spectral densities provide very useful information for the high frequency noise analysis of the devices; nevertheless, if one wants to compare the intrinsic noise behavior of the device with other structures, it is necessary to use normalized

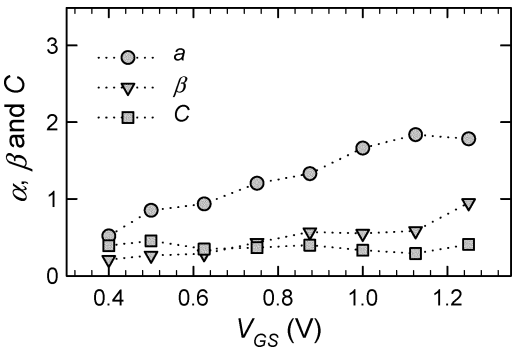

Fig. 7. Results for α, β, and C as a function of gate biasing.

parameters such as α, which is related to drain noise, β, associated to induced gate noise, and C, related to the correlation between noise sources [18]. These parameters incorporate not only the effect of intrinsic noise sources, but also the influence of dynamic parameters, following the equations given in [26] and [27]:

$$\alpha = \frac{S_{\mathrm{ID}}}{4K_BT|Y_{21}|} \tag{1}$$

$$\beta = \frac{S_{\mathrm{IG}}|Y_{21}|}{4K_BT|Y_{11}|^2} \tag{2}$$

$$C = \frac{\mathrm{Im}[S_{\mathrm{IGID}}]}{\sqrt{S_{\mathrm{IG}}S_{\mathrm{ID}}}} \tag{3}$$

where Y corresponds to the admittance parameters (1 and 2 correspond to the gate and to the drain terminals, respectively). As previously mentioned, the dynamic behavior of the devices (analyzed through the calculation of Y parameters) was satisfactorily evaluated in a previous work [14]. To complete the information concerning intrinsic noise sources, in Fig. 7 we show the results for α, β and C as a function of V_{GS} for $V_{\mathrm{DS}} = 1.5\,\mathrm{V}$, in saturation conditions. First of all, an important increase of α with the gate biasing is obtained as compared to van der Ziels prediction for a long channel device ($\sim$0.7), which is due to the enhancement of drain noise previously commented. On the other hand, it must be highlighted the increase of β for high gate biasing, related to the corresponding raise of induced gate noise because of the stronger capacitive coupling associated to the elevated concentration of carriers along the channel. Regarding the values of C, their average value is around 0.35, slightly lower than the result predicted by long-channel FET theory ($\sim$0.4) [18].

D. Simulated and Experimental Extrinsic Noise Parameters

Once the intrinsic noise sources and parameters provided by the MC simulation have been exhaustively analyzed, we will focus on the comparative study between experimental measurements and simulation results. For this purpose, the most adequate parameters are the usual four noise parameters ($\mathrm{NF}_{\mathrm{min}}$, R_n and complex Γ_{opt}), together with the associated gain G_{ass} that shall give more information to circuit designers. The process for calculating these parameters in the MC simulation is not an obvious task: the effect of extrinsic elements must be incorporated to the simulation results in order to allow a fair comparison with experimental data. For this purpose, we used

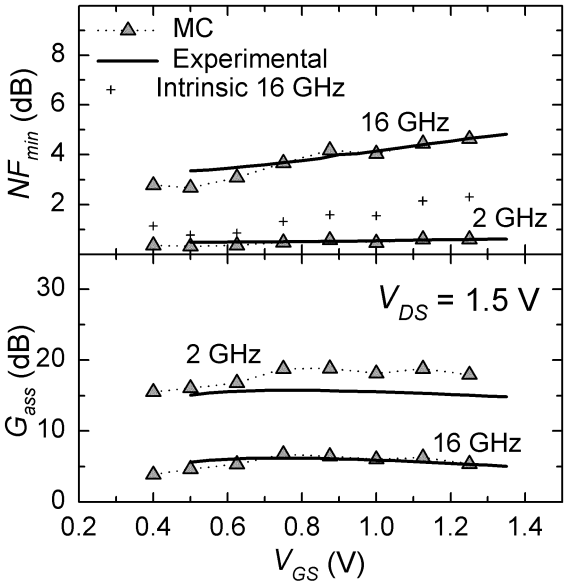

Fig. 8. Experimental measured data (solid lines) and MC results (symbols) for the minimum noise figure and associated gain at two different frequencies, 2 and 16 GHz. Crosshair symbols show the intrinsic values of NF_{min} (in dB) at 16 GHz.

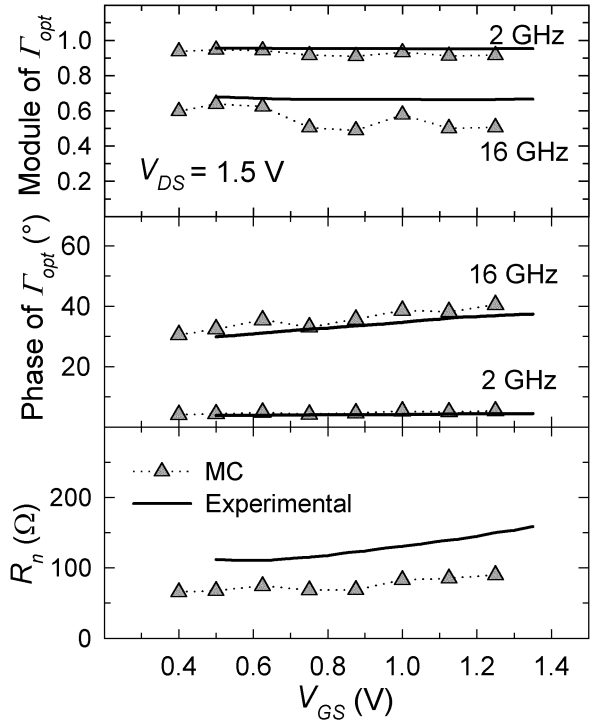

Fig. 9. Experimental measured data (solid lines) and MC results (symbols) for the module and phase of $\Gamma_{\rm opt}$ and the equivalent noise resistance R_n.

the modeling equations appearing in [28] which were elaborated starting from the expressions given in [29]; the method is based on the consideration of the device as a noise-free network with two short-circuit noise current generators at the input and the output (both correlated), together with the resistive noise current generators associated to the access resistances R_S, R_D and R_G. A scheme of the small-signal equivalent circuit considered (including parasitic elements) can be found in [14]. The procedure was satisfactorily tested in a previous published work for InP-based HEMT devices [30].

The values of the parasitic resistances were provided by the experimental extraction procedure, and are completely independent of the MC simulation: $R_S = 3.6\ \Omega$, $R_D = 3.3\ \Omega$ and $R_G = 34.0\ \Omega$. Taking into account the contribution of these access resistances, the results obtained for the minimum noise figure and the associated gain are shown in Fig. 8 for two different frequencies of operation, together with the experimental data corresponding to those same frequencies. As it can be observed, a good agreement is achieved between numerical simulations and experimental data for both the bias and frequency dependences. Excellent values for $NF_{\rm min}$ are obtained (minimum values of 0.4 and 2.7 dB at 2 and 16 GHz, respectively), which confirm the interest of these devices for analog high frequency applications. A linear dependence on frequency was found for $NF_{\rm min}$, in good accordance with the experimental measurements. As it can be observed in Fig. 8, $NF_{\rm min}$ tends to increase with the gate bias; by analyzing the expressions that provide $NF_{\rm min}$, we have checked that this is mainly due to the increase of drain noise (related to α). However, it is necessary to consider the contribution of induced gate noise in order to perform a reliable modeling of high frequency noise, as previously observed by other authors in the case of bulk devices [31]. Indeed, neglecting the gate current fluctuations (and the corresponding cross-correlation with the drain) leads to an important underestimation of the intrinsic values of the minimum noise figure. In our case, we found that the underestimation of the intrinsic noise factor ranges from 10 to 30% (up to 1.7 dB for the noise figure) at 16 GHz in the bias range considered.

Regarding the other noise FOMs, the results for the phase and module of $\Gamma_{\rm opt}$, together with the results for R_n (which was found to be practically frequency independent in the measurements) are shown in Fig. 9. It is noteworthy the accordance between experimental measurements and MC data for the optimum reflection coefficient. Nevertheless, in the case of R_n, although the bias dependence is quite well reproduced, the MC data show a clear underestimation of the total value of this quantity. The reasons for this disagreement are not clear at the present stage of our research. If the value of the parasitic gate resistance is increased, the simulation results are able to reproduce the measured extracted value for R_n. However, in this case the other noise parameters disagree with experimental results, which points toward other reasons for the discrepancy in the results of R_n. This discrepancy can not be attributed to a failure in our model, since drift-diffusion models applied to the study of the same devices under consideration in this work also found a similar underestimation of R_n [32]: a lack of technological data knowledge could be therefore at the origin of this discrepancy.

Since the EMC results provide the intrinsic behavior of the devices it is possible to evaluate the importance of parasitics on the final values of the main high-frequency noise FOMs. We found that parasitic elements account for around 40% of the total value of the noise factor at 16 GHz (the intrinsic values for $NF_{\rm min}$ at 16 GHz are plotted in Fig. 8, crosshair symbols). In the case of the associated gain, the importance of parasitic elements is crucial especially at elevated frequencies. These results address the importance of focusing on the minimization of

parasitic elements in order to fully profit from the exceptional intrinsic behavior of the device under test. Moreover, taking into account that parasitics can be reasonably predicted for a given technology when performing the downscaling, the simulator can be of great help to predict the tendency for the high-frequency noise behavior of future downscaled devices.

IV. Conclusion

A complete numerical and experimental investigation of the high-frequency noise behavior of deep-submicrometer FD SOI MOSFETs has been performed in this work. The information provided by the simulator, in terms of the internal quantities of interest, allows getting a proper understanding of the intrinsic noise sources. The bias dependence of the spectral density for drain current fluctuations has been deeply analyzed, paying attention to the onset of excess noise and the appearance of hot carriers. The study of local velocity fluctuations by means of the ensemble MC simulation has shown that carriers in the velocity overshoot region have a stronger intensity of velocity fluctuations and produce a significant local noise source. However, a final conclusion about its influence on the drain current noise would require the reliable evaluation of the adequate transfer field by means of deterministic approaches. The results have evidenced that in the case of the diffusive section, only for low $V_{\rm GS}$ a reasonable agreement is found between S_v and the prediction obtained by considering the diffusion coefficient corresponding to bulk material.

The detailed consideration of the real topology of the devices and the parasitic elements yields a general good agreement between the experimental measurements and the MC simulation for the most relevant noise FOMs, which confirms the reliability of the simulator for the study of high-frequency noise. It must also be mentioned the importance of a correct determination of induced gate noise in order to perform a reliable calculation of the minimum noise figure. Although the devices show an excellent behavior in the GHz frequency range of operation in terms of $\mathrm{NF}_{\rm min}$ and $G_{\rm ass}$, we have found that parasitic elements play a determinant role on the total noise generated by the device. In particular, the influence of parasitics on the minimum noise figure can be weighted of around 40% of the total value of the noise factor at 16 GHz, which may mask the excellent intrinsic performance of the device.

Appendix I

Most of the deterministic approaches for the study of noise are based in the consideration of ad hoc local current noise sources which are weighted by appropriate transfer fields (that can be determined i.e., by using Green functions) to obtain their contribution to the final current/voltage noise at the terminals, as in the so-called impedance field method (IFM). Within this framework, the local current noise source can be expressed in terms of the noise spectrum of the local velocity fluctuations [33]

$$S_{\rm in}(x,f)=\frac{q^2N(x)S_v(x,f)W}{dx} \tag{A1}$$

where q is the electron charge, $N(x)$ the local sheet carrier density, dx is the length of the local section, W the device width, $S_{\rm in}(x,f)$ the local noise source and $S_v(x,f)$ the local noise spectrum of velocity fluctuations, also know as velocity-fluctuation noise [18]

$$S_v(x,f)=4\int_0^\infty \delta v(t)\delta v(t+t')\cos(2\pi f t')dt' \tag{A2}$$

where δv corresponding to velocity fluctuation corresponding to one particle. According to Kubo [34], S_v is related to the high-frequency diffusion constant D through $S_v(x,f)=4\mathrm{Re}[D(x,f)]$, so in most cases the diffusion coefficient substitutes S_v in the definition of the local noise source.[1]

To determine the noise spectrum of current fluctuations at the drain terminal, it is necessary to take into account the influence of a transfer field

$$S'_{\rm ID}(f)=\int_0^L q^2\left|\frac{\partial A(x,f)}{\partial x}\right|^2 N(x)S_v(x,f)W\,dx \tag{A3}$$

where $A(x,f)$ is a dimensionless factor that, by analogy to the IFM method applied to the calculation of voltage noise, is usually known as the "impedance field" [9].

In our model (A.3) is not employed since $S\mathrm{v}(x,f)$ or $S_{\rm in}(x,f)$ are not necessary to determine the final current noise $S_{\rm ID}$, which is directly obtained from the MC values of the instantaneous current fluctuations at the terminals (see Section II). However, we may evaluate both $S_v(x,f)$ and $N(x)$ in two different regions of the channel in order to examine the values of the local current noise source (which can be of great interest for other groups using deterministic approaches) since in our model velocity fluctuations are naturally given without making any assumption about their origin, and hot carrier phenomena are "built-in" in the simulation. For this purpose, we have developed a procedure to determine, by means of the data provided by the EMC simulator, the value of $S_v(x,f)$, a quantity frequently used as the primary noise source in deterministic approaches. Special care was given to fulfill the requirements to correctly determine this noise source [36], [37]: the contribution of concentration fluctuations must be eliminated and the calculation must be performed in the absence of fluctuations of the self-consistent electric field. For this latter purpose, we "froze" the electric field by considering its average value after a preliminary simulation during 100 ps.

Let us consider a section Δx of the channel. Since the EMC simulation provides the instantaneous values of velocity for each simulated particle, we add all the values of longitudinal velocity (which is the velocity component that contributes to dc current and low frequency noise) of particles present in each section of the channel. The total sum is divided by the instantaneous number of particles $M(t)$ present in that section in order to obtain the average instantaneous velocity $v_m(t)$

$$v_m(t)=\frac{\sum_{i=1}^{M(t)} v_i(t)}{M(t)}. \tag{A4}$$

[1]To properly investigate nonequilibrium conditions or hot carrier phenomena, a possibility is to extend the use of the Einstein relation with the adequate consideration of the noise temperature and the mobility; this issue still remains a controversial question, yielding different solutions in the literature (i.e., [32], [35]).

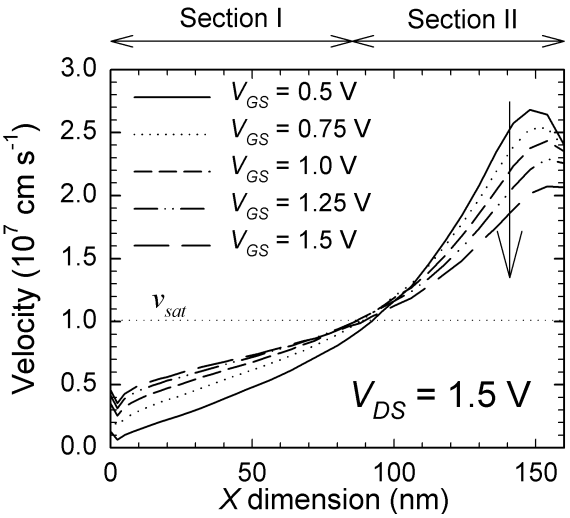

Fig. 10. Average longitudinal electron velocity in the channel for various values of $V_{\rm GS}$ ranging from 0.5 to 1.5 V at a fixed $V_{\rm DS} = 1.5$ V in saturation.

In this way, the contribution of the fluctuations of the number of particles is eliminated. The correlation function of the sum of the x-component velocities of the individual carriers is proportional to the number of particles simulated [38]. Therefore, to normalize the velocity fluctuations to one particle $[\delta v(t)]$ we multiply $\delta v_m(t)$ by the square root of the average number of particles. Afterwards, the spectral density of velocity fluctuations $S_v(x, f)$ is easily determined by using (A2). This methodology to compute $S_v(x, f)$ takes into account in a natural way the possible correlations between single carrier velocity fluctuations in each section, which could be relevant in the case of inhomogeneous samples.

In the results shown in the present work, we divided the channel in two different sections to analyze the contribution to velocity fluctuations of carriers: Section I corresponds to the part of the channel where carriers have a velocity below the saturation one, $v_{\rm sat}$, and Section II to the part of the channel where v is greater than $v_{\rm sat}$ in bulk material. Fig. 10 shows the values of average carrier velocity in the longitudinal dimension as a function of channel position for various values of $V_{\rm GS}$ at $V_{\rm DS} = 1.5$ V. The cross-correlations between velocity fluctuations in Sections I and II where found to be negligible in the frequency range of interest (this is, below 50 GHz) for all the values of $V_{\rm DS}$ and $V_{\rm GS}$ considered.

REFERENCES

[1] T. H. Lee and H. R. Rategh, "5-GHz CMOS wireless LANs," *IEEE Trans. Microw. Theory Tech.*, vol. 50, no. 1, pp. 268–280, Jan. 2002.

[2] C.-Y. Chang, J.-G. Su, S.-C. Wong, T.-Y. Huang, and Y.-C. Sun, "RF CMOS technology for MMIC," *Microelectron. Reliab.*, vol. 42, pp. 721–733, Apr. 2002.

[3] J. P. Colinge, *Silicon-on-Insulator Technology: Materials to VLSI*, 2nd ed. Norwell, MA: Kluwer, 1997.

[4] S. Cristoloveanu, "Silicon on insulator technologies and devices: from present to future," *Solid State Electron.*, vol. 45, pp. 1403–1411, Aug. 2001.

[5] G. G. Shahidi, "SOI technology for the GHz era," *IBM J. Res. Dev.*, vol. 46, no. 2/3, pp. 121–131, 2002.

[6] S. Donati, M. A. Alam, K. S. Krisch, S. Martin, M. R. Pinto, and H. H. Vuong, "Physics-based RF noise modeling of submicron MOSFETs," in *IEDM Tech. Dig.*, 1998, pp. 81–84.

[7] C. H. Chen and M. J. Deen, "Channel noise modeling of deep submicron MOSFETs," *IEEE Trans. Electron Devices*, vol. 49, pp. 1484–1487, Aug. 2002.

[8] A. J. Scholten, L. F. Tiemeijer, R. van Langevelde, R. J. Havens, A. T. A. Zegers-van Duijnhoven, and V. C. Venezia, "Noise modeling for RF CMOS circuit simulation," *IEEE Trans. Electron Devices*, vol. 50, no. 3, pp. 618–632, Mar. 2003.

[9] J.-S. Goo *et al.*, "An accurate and efficient high frequency noise simulation technique for deep submicron MOSFETs," *IEEE Trans. Electron Devices*, vol. 47, no. 12, pp. 2410–2419, Dec. 2000.

[10] S. Spedo and C. Fiegna, "Analysis of thermal noise in scaled MOS devices and RF circuits," *Solid State Electron.*, vol. 46, pp. 1933–1939, Nov. 2002.

[11] C. Jungemann *et al.*, "Hydrodynamic modeling of RF noise in CMOS devices," in *IEDM Tech. Dig.*, 2003, pp. 871–874.

[12] C. Jacoboni and P. Lugli, *The Monte Carlo Method for Semiconductor Device Simulation*. New York: McGraw-Hill, 1989.

[13] M. Vanmackelberg *et al.*, "0.25 μm fully depleted SOI MOSFETs for RF mixed analog-digital circuits, including a comparison with partially depleted devices with relation to high frequency noise parameters," *Solid State Electron.*, vol. 46, pp. 379–386, Mar. 2002.

[14] R. Rengel *et al.*, "Numerical and experimental study of a 0.25 μm fully depleted silicon-on-insulator MOSFET: static and dynamic radio-frequency behavior," *Semicond. Sci. Technol.*, vol. 17, pp. 1149–1156, 2002.

[15] R. Rengel, J. Mateos, D. Pardo, T. González, and M. J. Martín, "Monte Carlo analysis of dynamic and noise performance of submicron MOSFETs at RF and microwave frequencies," *Semicond. Sci. Technol.*, vol. 16, pp. 939–946, Nov. 2001.

[16] M. J. Martín, D. Pardo, and J. E. Velázquez, "Microscopic analysis of the influence of Ge profiles on the current-noise operation mode of $\rm n{-}Si/p{-}Si_{1-x}Ge_x$ heterostructures," *Semicond. Sci. Technol.*, vol. 15, pp. 277–285, Mar. 2000.

[17] M. J. Martín, J. E. Velázquez, and D. Pardo, "Analysis of current fluctuations in silicon $\rm pn^+$ and $\rm p^+n$ homojunctions," *J. Appl. Phys.*, vol. 79, pp. 6975–6981, May 1996.

[18] A. van der Ziel, *Noise in Solid State Devices and Circuits*. New York: Wiley, 1986.

[19] H. Kim, H. S. Min, T. W. Tang, and Y. J. Park, "An extended proof of the Ramo-Shockley theorem," *Solid State Electron.*, vol. 34, pp. 1251–1253, Nov. 1991.

[20] S. Babiker, A. Asenov, N. Cameron, S. P. Beaumont, and J. R. Barker, "Complete Monte Carlo RF analysis of "real" short-channel compound FETs," *IEEE Trans. Electron Devices*, vol. 45, no. 8, pp. 1644–1652, Aug. 1998.

[21] J. Mateos *et al.*, "Numerical and experimental analysis of the static characteristics and noise in ungated recessed MESFET structures," *Solid State Electron.*, vol. 39, pp. 1629–1636, Nov. 1996.

[22] M. J. Martín, S. Pérez, D. Pardo, and T. González, "Monte Carlo analysis of the noise behavior in Si bipolar junction transistors and SiGe heterojunction bipolar transistors at radio frequencies," *J. Appl. Phys.*, vol. 90, pp. 1582–1588, Aug. 2001.

[23] F. M. Klaassen and J. Prins, "Thermal noise of MOS transistors," *Phillips Res. Repts.*, pp. 505–514, 1967.

[24] D. P. Triantis, A. N. Birbas, and D. Kondis, "Thermal noise modeling for short-channel MOSFETs," *IEEE Trans. Electron Devices*, vol. 43, no. 11, pp. 1950–1955, Nov. 1996.

[25] G. Knoblinger, P. Klein, and H. Tiebout, "A new model for thermal channel noise of deep-submicron MOSFETs and its application in RF-CMOS design," *IEEE J. Solid-State Circuits*, vol. 36, no. 5, pp. 831–837, May 2001.

[26] R. A. Pucel, H. A. Haus, and H. Stanz, "Signal and noise properties of gallium arsenide microwave field effect transistors," *Adv. Electron. Electron Phys.*, vol. 38, pp. 195–263, 1975.

[27] F. Danneville, H. Happy, G. Dambrine, J. M. Belquin, and A. Cappy, "Microscopic noise modeling and macroscopic noise models: how good a connection?," *IEEE Trans. Electron Devices*, vol. 41, no. 5, pp. 779–786, May 1994.

[28] S. D. Greaves and R. T. Unwin, "Accurate noise characterization of short gate-length GaAs MESFETs and HEMTs for use in low noise optical receivers," *Microw. Opt. Tech. Lett.*, vol. 6, pp. 60–65, Jan. 1993.

[29] H. Rothe and W. Dahlke, "Theory of noisy fourpoles," *Proc. IRE*, vol. 44, no. 6, pp. 811–818, Jun. 1956.

[30] J. Mateos, T. González, D. Pardo, V. Höel, and A. Cappy, "Monte Carlo simulator for the design optimization of low-noise HEMTs," *IEEE Trans. Electron Devices*, vol. 47, no. 10, pp. 1950–1956, Oct. 2000.

[31] D. K. Shaeffer and T. H. Lee, "A 1.5-V, 1.5-GHz CMOS low noise amplifier," *IEEE J. Solid-State Circuits*, vol. 32, no. 5, pp. 745–759, May 1997.
[32] G. Pailloncy, B. Iñiguez, G. Dambrine, J.-P. Raskin, and F. Danneville, "Noise modeling in fully depleted SOI MOSFETs," *Solid State Electron.*, vol. 48, pp. 813–825, May 2004.
[33] A. Cappy and W. Heinrich, "High-frequency FET noise performance: a new approach," *IEEE Trans. Electron Devices*, vol. 36, no. 2, pp. 403–409, Feb. 1989.
[34] R. Kubo, "Statistical-mechanical theory of irreversible processes. I. General theory and simple applications to magnetic and conduction problems," *J. Phys. Soc. Japan*, vol. 12, pp. 570–586, Jun. 1957.
[35] K. Han, H. Shin, and K. Lee, "Analytical drain thermal noise current model valid for deep submicron MOSFETs," *IEEE Trans. Electron Devices*, vol. 51, no. 2, pp. 261–269, Feb. 2004.
[36] P. Shiktorov *et al.*, "Transfer-field methods for electronic noise in submicron semiconductor structures," *Rivista Nuovo Cimento*, vol. 24, pp. 1–71, 2001.
[37] ——, "On the spectral strength of the noise source entering the transfer impedance method," *Appl. Phys. Lett.*, vol. 71, pp. 3093–3095, Nov. 1997.
[38] J. Zimmermann and E. Constant, "Application of Monte Carlo techniques to hot carrier diffusion noise calculation in unipolar semiconducting components," *Solid State Electron.*, vol. 23, pp. 915–925, 1980.

Raúl Rengel was born in Tarrasa, Spain, in 1974. He received the B.S. and Ph.D. degrees in physics from the University of Salamanca, Salamanca, Spain, in 1997 and 2003, respectively.

From 1998 to 2000, he was with the Electronics Group, Department of Applied Physics, University of Salamanca as a Grant Holder. In 2001, he became Assistant Professor. He was a Postdoctoral Researcher during his six months at the Institute d'Electronique, de Microélectronique et de Nanotechnologies (IEMN), Villeneuve d'Ascq, Cedex, France. His main research activity is the MC modeling of electron transport in silicon devices, including the investigation of electronic noise processes and small-signal behavior in the high frequencies range in SOI MOSFET transistors and nonconventional silicon devices.

María Jesús Martín was born in Salamanca, Spain, in 1969. She received the B.S. and Ph.D. degrees in physics from the University of Salamanca, Salamanca, Spain, in 1992 and 1996, respectively.

Since 1992 she has been with the Electronics Group, Department of Applied Physics,University of Salamanca as a Grant Holder. Her graduate work focused on the simulation of transport and electronic noise in bipolar Si and SiGe structures. In 1995, she became Assistant Professor. She worked in 1997 and 1998 at the Electronic Components Technology and Materials (ECTM), Technological University of Delft, Delft, The Netherlands. This collaboration was in the field of designing MMIC amplifiers, for use in front-ends for GSM and DECT applications (using TEMIC's silicon germanium SiGe1 process). In 2002, she became Associate Professor of the University of Salamanca. Her current research interest is in the field of modeling of electronic transport and noise of submicrometer silicon devices.

Tomás González (M'05) was born in Salamanca, Spain, in 1967. He graduated in physics from the University of Salamanca, Salamanca, Spain, in 1990, where he received the Ph.D. degree in physics in 1994.

Since 1991 he has been working with the Electronics Group, Department of Applied Physics, University of Salamanca, with a Grant from the Spanish Education Ministry. In 1996 he became Associate Professor. His main research activity is in the field of electronic transport in semiconductor materials, electronic devices and mesoscopic structures, with special application to the modeling of electronic noise by microscopic approaches.

Javier Mateos was born in Salamanca, Spain, in 1970. He received the B.S. and Ph.D. degrees in physics from the University of Salamanca in 1993 and 1997, respectively.

Since 1993 he has been with the Electronics Group, Department of Applied Physics, University of Salamanca, as a Grant Holder. In 1996, he became Assistant Professor. He was with the Institut d'Electronique, de Microélectronique et de Nanotechnologies (IEMN), Lille, France for a year, where, in 2000, he became an Associate Professor. His present research interest is in the development of novel device concepts using ballistic transport, together with the modeling and optimization of the high-frequency and low-noise performance of ultrashort gate-length HEMTs.

Daniel Pardo was born in Valladolid, Spain, in 1946. He received the degree and the Ph.D. degree in physics from the University of Valladolid in 1971 and 1975, respectively.

From 1971 to 1981, he was with the Electronics Department, University of Valladolid, working on the characterization of semiconductor materials and modeling of semiconductor devices. He became Associate Professor in 1978. In 1981, he joined the Applied Physics Department, University of Salamanca, Salamanca, Spain, where he became a Full Professor and Head of the Electronics Group in 1983. His current research interest is the Monte Carlo simulation of semiconductor devices with special application to noise modeling.

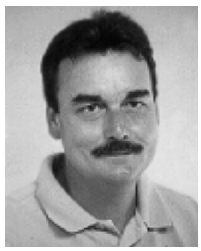

Gilles Dambrine (M'92) was born in Avion, France, on May 15, 1959. In 1986, he joined the Centre Hyperfréquences et Semiconducteurs, University of Lille, Lille, France, where he received the Ph.D. degree and the Habilitation à Diriger des Recherches (HDR) en Sciences degree in 1989 and 1996, respectively.

He was a Full Researcher at the Centre National de Recherche Scientifique (CNRS), France, between 1989 and 1999. He is now Professor of Electronics, University of Lille. His main research interests are concerned with the modeling and characterization of ultimate low-noise devices for application in millimeter- and sub-millimeterwave ranges. He is now the head of the "Advanced Nanometric Devices" (ANODE) group at Institut d'Electronique, de Microélectronique et de Nanotechnologie," Villeneuve d'Ascq, France. His research interests are oriented to the study of the microwave and millimeter-wave properties and applications of advanced silicon devices. He is author or coauthor of about 30 papers and 40 international communications and four book chapters in the field of microwave devices.

Prof. Dambrine is a member of the Technical Program Committee of the IEEE International Microwave Symposium and the European Microwave Conference since 2000. He is currently a reviewer in various IEEE TRANSACTIONS.

Jean-Pierre Raskin (M'97) was born in Aye, Belgium, in 1971. He received the Industrial Engineer degree from the Institut Supé;rieur Industriel d'Arlon, Belgium, in 1993, and the B.S. and Ph.D. degrees in applied sciences from the Université Catholique de Louvain (UCL), Louvain-la-Neuve, Belgium, in 1994 and 1997, respectively.

From 1994 to 1997, he was a Research Engineer at the Microwave Laboratory, UCL. He worked on the modeling, characterization, and realization of MMICs in SOI technology for low-power, low-voltage applications. In 1998, he joined the Electrical Engineering and Computer Science Department, The University of Michigan, Ann Arbor. He has been involved in the development and characterization of micromachining fabrication techniques for microwave and millimeter-wave circuits and microelectromechanical transducers/amplifiers working in hard environments. Since Jan. 2000, he is an Associate Professor at the Microwave Laboratory, UCL. His research interests are the modeling, wide-band characterization, and fabrication of advanced SOI MOSFETs as well as micro and nanofabrication of MEMS/NEMS sensors and actuators. He is a member of the Research Center in Micro and Nanoscopic Materials and Electronic Devices of the UCL. He is the author or coauthor of more than 200 scientific articles.

Dr. Raskin is an EuMA Associate Member.

François Danneville (M'98) was born in Ham, France, on March 16, 1964. He received the Ph.D. degree from the the Habilitation à Diriger des Recherches (HDR) and the Sciences degree from the Centre Hyperfréquences et Semiconducteurs, University of Lille, Lille, France, in 1991 and 1999, respectively.

In 1991, he was an Associate Professor, University of Lille, and his research has been carried out at the Institut d'Electronique, de Microélectronique et de Nanotechnologie (IEMN), Villeneuve d'Ascq, France, where he has studied the noise properties of III-V devices operating in linear and nonlinear regimes, for applications in centrimetric and millimetric ranges. In 1998, he held was a Visiting Professor in noise expertise at Hewlett-Packard (now Agilent), Electrical Engineering Division, Santa Rosa, CA. Since 2001, he is a Full Professor, University of Lille where his research at IEMN is oriented toward the study of the dynamic, noise, and nonlinear properties of MOSFET-based devices (including alternative architectures) and SiGe HBT as well as the design of low noise/low power circuits in millimetric wave range using SOI and SiGe BiCMOS technologies. He has authored or co-authored about 80 scientific international publications and communications. Heis an Editor for *Fluctuation and Noise Letters*.

Dr. Danneville has been Chairman of the Microwave Low Noise and Techniques Conference, the MTT-14 Technical Committee, and the IEEE Microwave Theory and Techniques Conference. He has been a member of several International Scientific or TP Committees (UPoN '99, SPIE FaN 2003, ICNF 2003 and 2005, and ICCDCS 2004). He was also the Chairman of the Noise in Devices and Circuits Conference, SPIE Fluctuations and Noise Symposium 2004, Maspalomas and Co-Chairman of the last Noise in Devices and Circuits Conference, which was part of the SPIE Fluctuations and noise Symposium held in Austin, TX.